

Similarity Solutions for the Flux-limited Keller–Segel System with Time-Varying Chemical Decay Rate

Ahmed Abbas Jaber Al-Furaiji and Ghorbanali Haghghatdoost* and Mustafa Bazghandi

Department of Mathematics, Azarbaijan Shahid Madani University, Tabriz, Iran

†

May 21, 2026

Abstract

We investigate a one-dimensional flux-limited Keller–Segel system (FLKS) in which the chemical decay rate is allowed to vary explicitly in time, a feature motivated by enzymatic regulation and environmental variability in chemotactic signalling. Treating the decay rate as an arbitrary function, we carry out a systematic Lie symmetry analysis of the resulting PDE system and employ equivalence transformations to perform a complete group classification, we identify the kernel symmetry algebra admitted for arbitrary decay functions and determine three distinguished cases that extend the symmetry algebra: constant decay rates, inverse-time (power-law) decay, and exponential decay. For each case, we construct an optimal system of subalgebras and derive the corresponding similarity reductions. Finally, we find some explicit solutions for our FLKS model. Our results provide a rigorous mathematical foundation for understanding which temporal decay patterns admit similarity reductions, thereby enabling analytical progress on flux-limited chemotaxis models with realistic time-varying degradation mechanisms.

Keywords: Lie symmetries; equivalence transformations; similarity solutions; flux-limited Keller–Segel system; chemotaxis.

AMS: 35Q92, 70G65, 76M60.

1 Introduction

The classical Keller–Segel (KS) model, while foundational in the mathematical study of chemotaxis, exhibits a critical mathematical deficiency: finite-time blow-up of cell densities under supercritical initial mass conditions. Such singularities are biologically implausible, as real cell populations remain bounded by volume exclusion, nutrient depletion, and other regulatory mechanisms. Preventing or regularizing these blow-up phenomena has thus become a central objective in chemotaxis modeling. To this end, various extensions have been proposed—including logistic growth terms [27], cross-diffusion mechanisms [4, 12], tempered fractional derivatives [9], and flux-limited formulations—each designed to restore global existence of solutions and produce physically meaningful long-time dynamics. Beyond the blow-up problem, the classical model suffers from an equally fundamental limitation in its representation of chemotactic transport. The classical model assumes velocity is linear ($\mathbf{u} = \chi \nabla v$), permitting unrestricted velocity growth as the magnitude of the gradient increases, failing to account for the inherent biomechanical constraints that govern cellular motility.

Recent advances have demonstrated that flux limitation corrects several core shortcomings of classical chemotaxis models: it enforces finite propagation speed in contrast to the infinite-speed transport of the classical Keller–Segel system, and yields aggregation dynamics consistent with empirical chemotaxis observations. Current research provide both rigorous mathematical analysis and computational evidence supporting the FLKS framework as a practical and robust model for chemotactic transport [5, 6, 15, 17, 18, 23].

In many chemotactic systems, the dominant mechanism controlling signal degradation is enzymatic. For example, in *Dictyostelium discoideum*, multiple phosphodiesterases (PDEs) regulate the hydrolysis of extracellular cAMP, and their expression levels vary substantially throughout the developmental cycle, causing strong

*Corresponding author, gorbanali@azaruniv.ac.ir

†E-mails: ahmedgon1234567@gmail.com, mostafabazghandi2001@gmail.com

temporal modulation of the effective decay rate $\kappa(t)$ [2, 8, 19]. Similar forms of enzyme-mediated regulation of chemoattractant breakdown occur in bacterial chemotaxis, where ligand-specific periplasmic enzymes adjust signal lifetimes in response to environmental conditions [1, 6]. These biochemical processes typically operate on developmental or stress-induced timescales, and therefore naturally induce time-dependent degradation dynamics. Consequently, enzymatic regulation provides a mechanistic basis for modeling κ as a non-constant function of time, highlighting the biological relevance of the generalized framework adopted in this study.

To accommodate these critical biological requirements, we analyze a generalized system where the chemotactic sensitivity κ is explicitly a function of time t . We restrict our analysis to the one-dimensional setting ($x \in \mathbb{R}$, $t \geq 0$), a choice motivated by several complementary considerations. First, one-dimensional models capture universal scaling behavior and intermediate asymptotics that persist across dimensions, while isolating the essential competition between diffusion, chemotactic flux, and time-dependent decay without the geometric complexities inherent in radial symmetry or multi-directional gradients. Second, this restriction ensures analytical tractability: the reduced ordinary differential equations obtained through symmetry methods admit exact or qualitative analysis that is generally unattainable in higher dimensions, thereby providing rigorous benchmark solutions for validating numerical schemes in two and three dimensions. Finally, many biologically relevant chemotaxis scenarios occur naturally in quasi-one-dimensional geometries, including bacterial chemotaxis in capillary tubes and microfluidic channels [16], aggregation streams in *Dictyostelium discoideum* [24], and cell migration along thin tissue strips or wound edges during tissue repair and morphogenesis [20]. We study the following one-dimensional flux-limited Keller–Segel system:

$$\begin{cases} u_t = Du_{xx} - (uf(v_x)v_x)_x, \\ \tau v_t = v_{xx} - \kappa(t)v + u, \end{cases} \quad (1)$$

where $D, \tau > 0$ are constants representing the diffusion coefficient, and time scale parameter, respectively, f is a bounded function that regulates chemotactic sensitivity, $\kappa(t)$ is an arbitrary function.

The function $f(s)$ is a flux-limiter governing the gradient-dependent chemotactic sensitivity. Unlike the classical Keller–Segel model, where the chemotactic velocity $u\nabla v$ becomes unbounded as $|\nabla v|$ increases, the flux-limited formulation imposes a finite maximal chemotactic speed. Specifically, $f(s)$ is assumed to be bounded and to satisfy $|f(s)s| \leq V_{\max}$, ensuring that steep gradients do not lead to biologically unrealistic transport.

Several flux-limiters have been proposed in the literature, each capturing distinct biophysical mechanisms. The algebraic limiter $\frac{s}{\sqrt{1+s^2}}$ captures generic saturation of chemotactic velocity [25, 28], the hyperbolic tangent limiter $\tanh(\frac{s}{s_0})$ provides smooth velocity regulation [11], and the Weber-Fechner form incorporates logarithmic sensing observed in *E. coli* [16].

Our objective is to perform a systematic classification of Lie symmetries with respect to arbitrary decay functions $\kappa(t)$, employing equivalence transformation theory to identify all admissible symmetry algebras. The foundational theory of group classification for nonlinear equations was proposed by Ovsiannikov [22], and has since been extended through both theoretical advances and widespread application to nonlinear evolution equations [13, 14, 26]. This approach enables us to determine which temporal decay patterns admit similarity reductions, thereby providing analytical progress on flux-limited chemotaxis models with realistic time-varying degradation mechanisms. To the best of our knowledge, no previous Lie symmetry analysis of flux-limited Keller–Segel (FLKS) systems with time-varying chemical decay exists in the literature.

Lie symmetry analysis has become an essential tool in the study of nonlinear partial differential equations, as it enables a systematic identification of the intrinsic geometric structures underlying differential equations. These structures can then be exploited to analyse differential invariants, construct exact or similarity solutions, and reveal the associated symmetry properties of the system (e.g. [3, 10]). Complementing this framework, equivalence transformations play a crucial role when investigating families of equations containing arbitrary functions or parameters, since they allow one to map the class of equations to canonical representatives, eliminate redundant cases, and clarify which structural features are essential for determining the behaviour of the model (e.g. [7]).

The remainder of this paper is structured as follows. Section 2 develops the equivalence transformation framework, derives the determining equations for the symmetry generators, and performs the group classification with respect to $\kappa(t)$. We establish the kernel symmetries admitted for arbitrary decay functions and identify the three distinguished functional forms that extend the symmetry algebra. Section 3 constructs an optimal system of subalgebras through which we systematically classify all non-equivalent symmetry reductions. Section 4 derives similarity reductions and invariant solutions corresponding to the admitted symmetries. Section 5

presents exact and semi-analytical solutions for representative cases, demonstrating the practical utility of the symmetry-based approach. Finally, We conclude with a discussion of the biological implications of our results and identify directions for future investigation.

2 Equivalence Transformations and Group Classification

The classical approach to Lie symmetry analysis determines the symmetries admitted by one specific differential equation system whose form is completely specified, meaning that all coefficients, parameters, and functions appearing in the equation are known and fixed. However, when a system contains arbitrary elements—functions or parameters that are not specified a priori—the appropriate framework is that of equivalence transformations [21, 26]. Rather than analyzing symmetries of one particular equation, we study transformations that map the entire class of equations (parametrized by the arbitrary element) into itself, thereby preserving the form of the system while potentially altering the arbitrary function. An *equivalence transformation* extends Lie symmetry to a *class of PDEs*, rather than a single fixed equation.

For the flux-limited Keller–Segel system (FLKS) under consideration, the chemical decay rate $\kappa(t)$ serves as the arbitrary element. To conduct a group classification, we seek point transformations of the extended space (x, t, u, v, κ) that preserve the structure of system (1) while transforming $\kappa(t)$ into another function $\tilde{\kappa}(\tilde{t})$.

2.1 Formulation of the Extended System

To implement the equivalence transformation method, we introduce κ as an additional dependent variable subject to the constraints that encode its defining property: κ depends only on time and is otherwise arbitrary. Specifically, we impose

$$\kappa_x = 0, \quad \kappa_u = 0, \quad \kappa_v = 0,$$

which together ensure that κ depends only on t and is otherwise arbitrary. The *extended* system in one spatial dimension then becomes

$$\begin{cases} \Delta_1 : & u_t = Du_{xx} - (uf(v_x) v_x)_x, \\ \Delta_2 : & \tau v_t = v_{xx} - \kappa(t)v + u, \\ \kappa_x = 0, & \kappa_u = 0, \quad \kappa_v = 0, \end{cases} \quad (2)$$

An equivalence transformation acts on this extended space through a point transformation

$$(x, t, u, v, \kappa) \mapsto (\tilde{x}, \tilde{t}, \tilde{u}, \tilde{v}, \tilde{\kappa}).$$

with the requirement that if (u, v, κ) satisfies system (2), then $(\tilde{u}, \tilde{v}, \tilde{\kappa})$ satisfies the same system in the transformed variables. The infinitesimal generator of such transformations takes the form

$$\mathbf{X}_E = \xi^t(x, t, u, v)\partial_t + \xi^x(x, t, u, v)\partial_x + \eta^u(x, t, u, v)\partial_u + \eta^v(x, t, u, v)\partial_v + \phi^\kappa(t, \kappa)\partial_\kappa, \quad (3)$$

where

$$\begin{aligned} \eta_t^u &= D_t(\eta^u) - u_t D_t(\xi^t) - u_x D_t(\xi^x), \\ \eta_x^u &= D_x(\eta^u) - u_t D_x(\xi^t) - u_x D_x(\xi^x), \\ \eta_t^v &= D_t(\eta^v) - v_t D_t(\xi^t) - v_x D_t(\xi^x), \\ \eta_x^v &= D_x(\eta^v) - v_t D_x(\xi^t) - v_x D_x(\xi^x), \\ \eta_{xx}^u &= D_x(\eta_x^u) - u_{tx} D_x(\xi^t) - u_{xx} D_x(\xi^x), \\ \eta_{xx}^v &= D_x(\eta_x^v) - v_{tx} D_x(\xi^t) - v_{xx} D_x(\xi^x), \\ &\dots, \end{aligned}$$

and the prolonged coefficient for κ_t is

$$\phi_t^\kappa = D_t(\phi) - \kappa_t D_t(\xi^t),$$

where there is no κ_x -term because $\kappa_x = 0$ by the constraints; D_t and D_x are total derivatives. The second prolongation $\mathbf{X}_E^{(2)}$ acts on

$$\{u_t, u_x, u_{xx}, v_t, v_x, v_{xx}, \kappa_t, \kappa_x\}.$$

If we find transformations that map one form of $\kappa(t)$ into another, we can classify all functions $\kappa(t)$ that produce additional symmetries. This leads to the *group classification* of the class of PDEs. Applying the second prolongation $\mathbf{X}_E^{(2)}$ on $\kappa_x = 0$, $\kappa_u = 0$, $\kappa_v = 0$ and using the invariance condition, we obtain

$$\begin{aligned}\xi_\kappa^t &= 0, & \xi_\kappa^x &= 0, & \eta_\kappa^u &= 0, & \eta_\kappa^v &= 0, \\ \phi_x &= 0, & \phi_u &= 0, & \phi_v &= 0,\end{aligned}\tag{4}$$

From the diffusion terms Du_{xx} , v_{xx} , and the requirement that f is an arbitrary function of v_x , the time coefficient depends only on time, and the space coefficient is linear in x :

$$\begin{aligned}\xi_x^t &= 0, & \xi_u^t &= 0, & \xi_v^t &= 0, \\ \xi_{uu}^x &= 0, & \xi_{uv}^x &= 0, & \xi_{vv}^x &= 0, & \xi_{xu}^x &= 0, & \xi_{xv}^x &= 0, & \xi_{xx}^x &= 0,\end{aligned}\tag{5}$$

Consequently, we have

$$\xi^t = \xi^t(t), \quad \xi^x = \frac{1}{2}\dot{\xi}^t(t)x + k_1(t)\tag{6}$$

Due to the nonlinear coupling in the flux term $(uf(v_x)v_x)_x$, the projective symmetries are lost, forcing ξ^t to be affine:

$$\begin{aligned}\xi^t(t) &= c_1t + c_2 \\ \xi^x(x) &= \frac{1}{2}c_1x + c_3\end{aligned}$$

where c_1, c_2, c_3 are arbitrary constants.

From the flux term's dependence on u and v_x and the arbitrariness of f , we get linearity of η^u and η^v in u and v :

$$\begin{aligned}\eta_{uu}^u &= 0, & \eta_{uv}^u &= 0, & \eta_{vv}^u &= 0, \\ \eta_{uu}^v &= 0, & \eta_{uv}^v &= 0, & \eta_{vv}^v &= 0,\end{aligned}$$

which implies:

$$\eta^u = \alpha(x, t)u + \beta(x, t), \quad \eta^v = \gamma(t)v + \delta(x, t)$$

So after the structural equations, the generator takes the reduced form

$$\mathbf{X}_E = \xi^t(t) \partial_t + (a(t)x + b(t)) \partial_x + (\alpha u + \beta) \partial_u + (\gamma v + \delta) \partial_v + \phi(t, \kappa) \partial_\kappa.$$

2.2 Determining Equations

Applying the second prolongation $X_E^{(2)}$ to the differential equations Δ_1 and Δ_2 and requiring that the prolonged generator annihilate these equations yields the full system of determining equations.

Applying $X_E^{(2)}$ to Δ_1 , substituting u_t from $\Delta_1 = 0$, gives the determining equations

$$2a(t) = \xi_t^t(t), \quad \beta_t - D\beta_{xx} = 0, \quad \alpha_t - D\alpha_{xx} = 0$$

No mixing of higher x -derivatives in flux part (coefficients of v_{xx} , f , f') forces the generator to preserve the structure

$$\alpha_x = 0, \quad \delta_x \text{ free,}$$

plus the restriction that no extra dependence on v_x is generated. In particular, the coefficients of

$$uf(v_x), \quad uf'(v_x), \quad u_x f(v_x), \quad u_x f'(v_x),$$

all vanish separately. This yields

$$\gamma_x = 0, \quad \gamma_u = 0, \quad \gamma_v = 0 \quad \Rightarrow \quad \gamma = \gamma(t),$$

Collecting, from Δ_1 we get the determining equations:

$$\begin{aligned}\xi_t^t &= 2a(t), \\ \alpha_x &= 0, \quad \gamma = \gamma(t), \\ \alpha_t - D\alpha_{xx} &= 0, \quad \beta_t - D\beta_{xx} = 0.\end{aligned}$$

Applying $X_E^{(2)}$ to Δ_2 and using the invariance condition, gives the determining equations

$$\begin{aligned}\xi_t^t &= 2a(t), \quad \alpha = 1, \\ \tau \gamma_t + \xi^t \dot{\kappa} + \kappa(\xi_t^t + \gamma - \tau \xi_t^t) &= 0, \\ \tau \delta_t - \delta_{xx} + \kappa(t)\delta - \beta &= 0.\end{aligned}$$

2.3 Group Classification

To obtain the specific forms of $\kappa(t)$ from the determining equations, we must solve the *classifying condition*. This is a specific subset of the full determining equations that isolates the time-dependent parameter $\kappa(t)$, which here it is

$$\tau \gamma_t(t) + \xi^t(t) \dot{\kappa}(t) + \kappa(t)(\xi_t^t(t) + \gamma(t) - \tau \xi_t^t(t)) = 0, \quad (7)$$

Equation (7) acts as a first-order linear non-homogeneous ODE for the classification function $\kappa(t)$. For $\kappa(t)$ to admit the fundamental symmetry extensions (such as scaling or translational invariant forms) rather than arbitrary driven solutions, the non-homogeneous term must vanish. Assuming $\tau \neq 0$ (for non-trivial time extensions), this requires:

$$\gamma_t(t) = 0 \implies \gamma(t) = \lambda,$$

where λ is an arbitrary constant. Consequently, Eq. (7) is reduced to

$$\xi^t(t) \dot{\kappa}(t) + (\xi_t^t(t) - \lambda)\kappa(t) = 0,$$

which is the ODE for $\kappa(t)$ used in the classification.

We identify three distinct cases for the chemical decay rate $\kappa(t)$:

Case 1: Arbitrary $\kappa(t)$ (Kernel Symmetries). If $\kappa(t)$ is arbitrary, then $\xi^t = 0$ and $\xi_t^t = 0$. The only admitted symmetries are space translations:

$$X_1 = \partial_x.$$

Case 2: Constant Decay Rate $\kappa(t) = \kappa_0$. If $\kappa(t)$ is a constant, then $\dot{\kappa} = 0$. This allows time translation symmetry ($\xi^t = 1$) and specific scaling symmetries.

$$X_2 = \partial_t, \quad X_3 = \partial_x.$$

Case 3: Inverse Time (Power Law) Decay $\kappa(t) = \frac{\mu}{t}$ Substituting $\kappa(t) = \mu t^{-1}$ into the classifying relation with $\xi^t = c_1 t$ (scaling in time):

$$c_1 t(-\mu t^{-2}) + c_1(\mu t^{-1}) + \dots = 0$$

This form admits a dilation symmetry X_D that scales time and the decay rate simultaneously. The admitted operators are:

$$X_D = t\partial_t + \frac{1}{2}x\partial_x + \eta^u(x, t, u, v)\partial_u + \eta^v(x, t, u, v)\partial_v, \quad (8)$$

where the u - and v -components of the generator (8) are some linear combinations of $u\partial_u$ and $v\partial_v$, and for the purpose of *classifying* $\kappa(t)$ they are not needed, so they were suppressed.

Case 4: Exponential decay The exponential form $\kappa(t) = \kappa_0 e^{\lambda t}$ is obtained by solving the determining equation under the assumption that the system possesses a symmetry generated by time translation combined with scaling:

$$X = \partial_t - \lambda v \partial_v.$$

Table 1: Classification of Lie symmetries for system (1).

Case	Decay Function $\kappa(t)$	Admitted Operators	Physical Interpretation
I	$\forall \kappa(t)$	$X_1 = \partial_x$	Space Translation (Homogeneity of space)
II	κ_0 (const)	$X_1, X_2 = \partial_t$	Time Translation (Autonomous system)
III	μt^{-1}	$X_1, X_3 = t\partial_t + \frac{x}{2}\partial_x + \dots$	Scaling / Self-similar degradation
IV	$e^{\lambda t}$	$X_1, X_4 = \partial_t - \lambda v \partial_v$	Exponential decay/growth compensation

Solving the determining equations for these specific forms yields a complete classification of Lie symmetries for the system (1), as presented in Table 1.

This classification confirms that while the arbitrary time-varying decay $\kappa(t)$ generally breaks the time-translation symmetry of the classical KS model, specific functional forms—particularly the power-law decay $\kappa(t) \sim 1/t$ —preserve a self-similar structure that allows for the construction of similarity solutions.

3 Optimal System of Subalgebras

Having established the complete group classification in Section 2, we now construct optimal systems of one-dimensional subalgebras for each distinguished case of κ . The optimal system provides a minimal set of inequivalent similarity reductions, thereby avoiding redundant calculations while ensuring that all physically distinct solutions are captured. We employ the adjoint representation method to systematically classify the subalgebras up to conjugacy.

Case I : Arbitrary $\kappa(t)$

For an arbitrary time-dependent decay rate $\kappa(t)$, the admitted symmetry algebra reduces to the one-dimensional kernel:

$$\mathfrak{g}^{(I)} = \text{span}\{X_1\}, \quad X_1 = \partial_x.$$

This kernel algebra reflects only the translational invariance in space, which persists regardless of the temporal variation in the chemical decay rate. Since $\mathfrak{g}^{(I)}$ is one-dimensional and Abelian, there exists only a single nontrivial subalgebra up to scalar multiplication.

$$\mathcal{A}_{\text{opt}}^{(I)} = \{\langle X_1 \rangle\}.$$

Case II : Constant $\kappa(t) = \kappa_0$

When the chemical decay rate is constant, the system becomes autonomous and admits an additional time-translation symmetry. The symmetry algebra becomes two-dimensional:

$$\mathfrak{g}^{(II)} = \text{span}\{X_1, X_2\}, \quad X_1 = \partial_x, \quad X_2 = \partial_t.$$

with commutation relation

$$[X_1, X_2] = 0.$$

Thus $\mathfrak{g}^{(II)}$ forms a two-dimensional Abelian Lie algebra. The adjoint action is trivial, reducing the classification of one-dimensional subalgebras to the consideration of all nonequivalent linear combinations of the basis generators.

A general one-dimensional subalgebra is spanned by

$$X = aX_1 + bX_2, \quad (a, b) \neq (0, 0).$$

Under scalar multiplication, we may normalize either coefficient to unity, yielding a one-parameter family of inequivalent directions. To obtain a discrete optimal system, we select representative generators corresponding to the limiting cases and the generic combination.

$$\mathcal{A}_{\text{opt}}^{(II)} = \left\{ \langle X_1 \rangle, \langle X_2 \rangle, \langle X_1 + \alpha X_2 \rangle \mid \alpha \in \mathbb{R} \setminus \{0\} \right\}.$$

Case III : Power-law $\kappa(t) = \frac{\mu}{t}$

The inverse-time decay case admits a scaling symmetry that captures the self-similar structure of the degradation mechanism. The symmetry algebra is

$$\mathfrak{g}^{(III)} = \text{span}\{X_1, X_3\},$$

where

$$X_1 = \partial_x, \quad X_3 = t\partial_t + \frac{1}{2}x\partial_x + \eta^u(x, t, u, v)\partial_u + \eta^v(x, t, u, v)\partial_v.$$

The precise form of the coefficients η_u and η_v depends on the specific flux-limiting function f .

Consider a general one-dimensional subalgebra spanned by

$$X = aX_1 + bX_3.$$

- If $b \neq 0$: scale X so $b = 1$: $X = X_3 + cX_1$. The adjoint action of $\exp(\varepsilon X_3)$ transforms this generator according to

$$\text{Ad}(\exp(\varepsilon X_3))(X_3 + cX_1) = X_3 + ce^{-\varepsilon/2}X_1.$$

By choosing $\varepsilon = 2 \ln |c|$, we can map any nonzero c to $c = 1$ or eliminate the X_1 term entirely. Thus all such subalgebras are conjugate to $\langle X_3 \rangle$.

- If $b = 0$: We have $X = aX_1$, which reduces to $\langle X_1 \rangle$.

Consequently, the optimal system is

$$\mathcal{A}_{\text{opt}}^{(III)} = \{\langle X_1 \rangle, \langle X_3 \rangle\}.$$

The generator X_1 corresponds to spatially homogeneous reductions, while X_3 yields self-similar solutions adapted to the power-law temporal structure of the decay rate $\kappa(t) = \frac{\mu}{t}$. These self-similar reductions are of particular interest for analyzing long-time asymptotic behavior and intermediate asymptotics of the flux-limited system.

Case IV : Exponential $\kappa(t) = \kappa_0 e^{\lambda t}$

For exponential temporal decay (or growth, depending on the sign of λ), the symmetry algebra is

$$\mathfrak{g}^{(IV)} = \text{span}\{X_1, X_4\},$$

where

$$X_1 = \partial_x, \quad X_4 = \partial_t - \lambda v \partial_v.$$

The generator X_4 combines time translation with a linear rescaling of the chemical concentration v , reflecting the exponential time dependence of the decay rate. The commutation relation is

$$[X_1, X_4] = 0.$$

Therefore $\mathfrak{g}^{(IV)}$ is again a two-dimensional Abelian algebra. The classification of one-dimensional subalgebras proceeds identically to Case II, with trivial adjoint action and a one-parameter family of inequivalent directions.

The optimal system is

$$\mathcal{A}_{\text{opt}}^{(IV)} = \left\{ \langle X_1 \rangle, \langle X_4 \rangle, \langle X_1 + \alpha X_4 \rangle \mid \alpha \in \mathbb{R} \setminus \{0\} \right\}.$$

The optimal systems constructed above provide a complete and nonredundant catalog of inequivalent similarity reductions for each case of the time-dependent decay rate $\kappa(t)$. The results are summarized in Table 2.

In Section 4, we apply these optimal systems to derive explicit similarity variables and reduced ordinary differential equations for each admitted symmetry, thereby enabling the construction of exact and approximate solutions for the flux-limited Keller–Segel system with time-dependent chemical decay.

Table 2: Classification of cases and corresponding optimal 1D subalgebras.

Case	$\kappa(t)$	Optimal 1D System
I	arbitrary $\kappa(t)$	$\langle X_1 \rangle$
II	κ_0 (const.)	$\langle X_1 \rangle, \langle X_2 \rangle, \langle X_1 + \alpha X_2 \rangle$
III	$\frac{\mu}{t}$ (power-law)	$\langle X_1 \rangle, \langle X_3 \rangle$
IV	$\kappa_0 e^{\lambda t}$ (exponential)	$\langle X_1 \rangle, \langle X_4 \rangle, \langle X_1 + \alpha X_4 \rangle$

4 Symmetry Reductions

In this section we derive group-invariant reductions of the flux-limited Keller–Segel system (1) corresponding to the optimal systems obtained in Section 3. For each admissible generator, we determine the invariants, construct the associated similarity ansatz, and obtain the reduced system governing the invariant solutions. The Lie symmetry approach yields the general form of the solutions, regardless of the flux. In the subsequent analysis, we utilize the specific properties of the Weber-Fechner and the hyperbolic tangent flux limiters to demonstrate the power of these reductions by obtaining explicit, fully analytical solutions (reductions to quadratures) that serve as valuable benchmarks.

4.1 Case I: Arbitrary $\kappa(t)$

For an arbitrary time-dependent decay rate $\kappa(t)$, the admitted symmetry algebra reduces to the spatial translation generator $X_1 = \partial_x$. The optimal system consists of the single subalgebra X_1 , corresponding to spatially homogeneous solutions.

Reduction via X_1 : The invariance condition $X_1[u] = 0$ and $X_1[v] = 0$ implies $u_x = v_x = 0$, yielding the ansatz

$$u(x, t) = U(t), \quad v(x, t) = V(t).$$

Under this reduction, all spatial derivatives vanish: $u_{xx} = v_{xx} = v_x = 0$. The flux term $u f(|\nabla v|) \nabla v$ identically vanishes, and system (1) reduces to the following coupled ODEs:

$$\begin{cases} U'(t) = 0, \\ \tau V'(t) = -\kappa(t) V(t) + U(t). \end{cases} \quad (9)$$

The first equation immediately integrates to $U(t) = c_0$, where c_0 is an arbitrary constant representing the conserved total cell population. Substituting into the second equation yields a first-order linear inhomogeneous ODE for $V(t)$:

$$\tau V'(t) + \kappa(t) V(t) = c_0. \quad (10)$$

4.2 Case II : $\kappa(t) = \kappa_0$ (constant)

When the chemical decay rate is constant, the optimal system comprises three inequivalent subalgebras: X_1 , X_2 , and $X_1 + \alpha X_2$, where $X_1 = \partial_x$ and $X_2 = \partial_t$.

4.2.1 Reduction via X_1 :

This case is identical to Case I with $\kappa(t)$ replaced by the constant κ_0 . The reduced system is

$$\begin{cases} U'(t) = 0, \\ \tau V'(t) = -\kappa_0 V(t) + U(t). \end{cases} \quad (11)$$

This solution describes relaxation to a steady state $V^\infty = \frac{c_0}{\kappa_0}$ determined by the balance between cell production and chemical decay.

4.2.2 Reduction via X_2 :

The time-translation generator $X_2 = \partial_t$ yields steady-state solutions satisfying $u_t = v_t = 0$. The ansatz

$$u(x, t) = U(x), \quad v(x, t) = V(x).$$

reduces system (1) to the autonomous boundary-value problem

$$\begin{cases} 0 = DU''(x) - \frac{d}{dx}(U(x) f(V'(x)) V'(x)), \\ 0 = V''(x) - \kappa_0 V(x) + U(x). \end{cases} \quad (12)$$

These equations describe stationary spatial patterns in which diffusion, chemotactic flux, and chemical production/decay are in balance. The structure of solutions depends critically on the choice of flux-limiting function f and the boundary conditions imposed at the domain boundaries.

4.2.3 Reduction via $\langle X_1 + \alpha X_2 \rangle$:

The combined generator $X = \partial_x + \alpha \partial_t$ describes traveling-wave solutions propagating with constant speed α . The characteristic equations

$$\frac{dx}{1} = \frac{dt}{\alpha} \Rightarrow t - \alpha x = \text{const},$$

yield the similarity variable

$$y = t - \alpha x, \quad (13)$$

under which the solution takes the form

$$u(x, t) = U(y), \quad v(x, t) = V(y).$$

Computing derivatives with respect to (x, t) in terms of derivatives with respect to y :

$$\begin{aligned} y_t &= 1, & y_x &= -\alpha, \\ u_t &= U_y, & u_x &= -\alpha U_y, & u_{xx} &= \alpha^2 U_{yy}, \\ v_t &= V_y, & v_x &= -\alpha V_y, & v_{xx} &= \alpha^2 V_{yy}. \end{aligned}$$

The flux term becomes

$$\begin{aligned} J &:= u f(v_x) v_x = U(y) f(-\alpha V_y) (-\alpha V_y), \\ J_x &= \frac{dJ}{dx} = \frac{dJ}{dy} y_x = -\alpha \frac{d}{dy} \left(U f(-\alpha V_y) (-\alpha V_y) \right). \end{aligned}$$

Substituting into system (1) yields the traveling-wave ODEs

$$\begin{cases} U_y = D\alpha^2 U_{yy} - \alpha \frac{d}{dy} \left(U f(-\alpha V_y) (-\alpha V_y) \right), \\ \tau V_y = \alpha^2 V_{yy} - \kappa_0 V + U. \end{cases} \quad (14)$$

4.3 Case III : $\kappa(t) = \frac{\mu}{t}$ (power-law decay)

The inverse-time decay case admits the scaling symmetry $X_3 = t\partial_t + \frac{1}{2}x\partial_x + au\partial_u + bv\partial_v$, where the constants a and b are determined by the flux structure. The optimal system consists of X_1 and X_3 .

4.3.1 Reduction via X_1 :

As in previous cases, spatial homogeneity yields

$$\begin{cases} U'(t) = 0, \\ \tau V'(t) = -\frac{\mu}{t} V(t) + U(t). \end{cases} \quad (15)$$

4.3.2 Reduction via X_3 :

The scaling generator X_3 reflects the self-similar structure induced by the power-law decay. The invariants of the (x, t) -component $X_3^{(tx)} = t\partial_t + \frac{1}{2}x\partial_x$ determine the similarity variable

$$\xi = \frac{x}{\sqrt{t}}.$$

To construct the full similarity ansatz, we incorporate the u - and v -scaling components of X_3 . Dimensional analysis and invariance under X_3 suggest the power-law scaling

$$u(x, t) = t^p U(\xi), \quad v(x, t) = t^q V(\xi), \quad \xi = \frac{x}{\sqrt{t}},$$

To ensure a genuinely flux-limited response while retaining logarithmic sensing, we adopt the bounded function

$$F(S) = V_{\max} \tanh(\ln(1 + aS^2)),$$

where $V_{\max} > 0$ denotes the maximal chemotactic speed and $a > 0$ controls the sensitivity of the response. The outer hyperbolic tangent guarantees the bound

$$|F(S)| \leq V_{\max},$$

while the inner logarithmic dependence preserves the tanh-squared limiter sensory structure.

Here we select the exponents p and q so that, after substitution of the similarity ansatz, the transformed equations contain no explicit t -dependence. Equivalently, the t -factors multiplying the reduced terms must cancel so that the resulting profiles depend only on ξ .

Choosing the similarity exponents

$$p = -\frac{1}{2}, \quad q = \frac{1}{2},$$

eliminates the explicit time dependence of the flux term because

$$v_x = V'(\xi).$$

Consequently,

$$F(v_x) = V_{\max} \tanh(\ln(1 + aV'^2)).$$

Substituting the similarity forms into the first equation in system (1) and multiplying by t yields

$$U'' - \partial_\xi(UV_{\max}\Phi(V')) = pU - \frac{1}{2}\xi U',$$

where

$$\Phi(V') = \tanh(\ln(1 + aV'^2)).$$

Using $p = -\frac{1}{2}$ this equation becomes

$$U'' - \partial_\xi(UV_{\max}\Phi(V')) = -\frac{1}{2}U - \frac{1}{2}\xi U'.$$

The second equation in system (1) reduces to

$$V'' - \frac{1}{2}\xi V' + qV = U,$$

and with $q = \frac{1}{2}$ we obtain

$$V'' - \frac{1}{2}\xi V' + \frac{1}{2}V = U.$$

Hence the similarity reduction of the system leads to the coupled ordinary differential equations

$$\begin{cases} U'' - \partial_\xi(UV_{\max}\Phi(V')) = -\frac{1}{2}U - \frac{1}{2}\xi U', \\ V'' - \frac{1}{2}\xi V' + \frac{1}{2}V = U. \end{cases} \quad (16)$$

with

$$\Phi(V') = \tanh(\ln(1 + aV'^2)).$$

The function $\Phi(V')$ represents a bounded tanh-squared limiter chemotactic response. For small gradients V' the response behaves approximately logarithmically, while for large gradients the hyperbolic tangent ensures saturation of the chemotactic velocity at V_{\max} . This formulation reconciles the tanh-squared limiter sensing with the physically motivated requirement of flux limitation.

4.4 Case IV : $\kappa(t) = \kappa_0 e^{\lambda t}$ (exponential)

The exponential decay case admits the combined generator $X_4 = \partial_t - \lambda v \partial_v$, which encodes the time-dependent rescaling necessary to compensate for exponential growth or decay. The optimal system consists of X_1 , X_4 , and $X_1 + \alpha X_4$.

4.4.1 Reduction via X_1 :

Spatial homogeneity yields

$$\begin{cases} U'(t) = 0, \\ \tau V'(t) = -\kappa_0 e^{\lambda t} V(t) + U(t). \end{cases} \quad (17)$$

4.4.2 Reduction via X_4 :

The invariance conditions $X_4[u] = u_t = 0$ and $X_4[v] = v_t - \lambda v = 0$ imply

$$u(x, t) = U(x), \quad v(x, t) = e^{\lambda t} V(x).$$

Computing derivatives:

$$u_t = 0, \quad u_{xx} = U''(x), \quad v_t = \lambda e^{\lambda t} V(x), \quad v_x = e^{\lambda t} V'(x), \quad v_{xx} = e^{\lambda t} V''(x).$$

The flux term is

$$J = U(x) f(e^{\lambda t} V'(x)) e^{\lambda t} V'(x),$$

Substituting into system (1):

$$\begin{cases} 0 = DU''(x) - \frac{d}{dx} \left(U(x) f(e^{\lambda t} V'(x)) e^{\lambda t} V'(x) \right), \\ \tau \lambda V = V'' - \kappa_0 V + e^{-\lambda t} U(x). \end{cases} \quad (18)$$

These equations retain explicit time dependence through the exponential factors. Full time-independence requires additional constraints from the determining equations, which may restrict the flux function f or impose specific relationships among the parameters D , α , κ_0 , and λ . Nevertheless, this reduction captures the qualitative feature that exponential temporal decay can be absorbed into an exponential rescaling of the chemical concentration, decoupling the time evolution from spatial pattern formation.

4.4.3 Reduction via $X_1 + \alpha X_4$:

The combined generator $X = \partial_x + \alpha \partial_t - \alpha \lambda v \partial_v$ describes traveling waves with decay compensation. The characteristic system is

$$\frac{dx}{1} = \frac{dt}{\alpha} = \frac{dv}{-\alpha \lambda v}.$$

From the first equality, we obtain the traveling-wave coordinate

$$y = t - \alpha x$$

From the second equality:

$$\frac{dv}{v} = -\lambda dt \Rightarrow v e^{\lambda t} = \Phi(y),$$

where Φ is an arbitrary function of y . This motivates the ansatz

$$u(x, t) = U(y), \quad v(x, t) = e^{-\lambda t} V(y), \quad y = t - \alpha x.$$

Flux term:

$$\begin{aligned} J &:= uf(v_x)v_x = U(y) f(-\alpha e^{-\lambda t} V_y) (-\alpha e^{-\lambda t} V_y), \\ J_x &= \frac{\partial J}{\partial y} y_x = -\alpha \frac{d}{dy} \left(U f(-\alpha e^{-\lambda t} V_y) (-\alpha e^{-\lambda t} V_y) \right). \end{aligned}$$

The reduced system is:

$$\begin{cases} U_y = D\alpha^2 U_{yy} - \alpha \frac{d}{dy} \left(U f(-\alpha e^{-\lambda t} V_y) (-\alpha e^{-\lambda t} V_y) \right), \\ \tau(V_y - \lambda V) = \alpha^2 V_{yy} - \kappa_0 V + e^{\lambda t} U(y). \end{cases} \quad (19)$$

As in the previous case, complete elimination of time dependence requires specific parameter relationships; however, the reduction isolates the essential coupling between traveling-wave dynamics and exponential decay/growth mechanisms.

In Section 5, we exploit these reduced systems to construct explicit analytical solutions for specific choices of the flux-limiting function f , thereby demonstrating the power of the symmetry-based approach for obtaining closed-form solutions to this biologically relevant chemotaxis model.

5 Explicit Solutions

In this section we construct explicit solutions associated with the symmetry reductions for each distinguished case in Section 4, and interpret them in a biologically meaningful way. Each solution family can be viewed as a *canonical dynamical scenario* for a chemotactic population under a given temporal regulation of the chemoattractant decay rate $\kappa(t)$.

5.1 Case I: arbitrary $\kappa(t)$

We now construct explicit analytical solutions for the spatially homogeneous reductions corresponding to the generator $X_1 = \partial_x$. These solutions apply to all distinguished cases of the decay function $\kappa(t)$ and require no assumptions on the flux-limiting function f , since all spatial derivatives vanish identically under the X_1 -invariant ansatz $u(x, t) = U(t), v(x, t) = V(t)$. Equation (10) is a linear first-order ODE. This equation can be rewritten in standard form as

$$V'(t) + a(t) V(t) = b(t), \quad a(t) = \frac{\kappa(t)}{\tau}, \quad b(t) = \frac{C}{\tau}.$$

Employing the method of integrating factors, we define

$$\mu(t) = \exp\left(\int^t a(s) ds\right) = \exp\left(\frac{1}{\tau} \int^t \kappa(s) ds\right).$$

Multiplying both sides of the equation by $\mu(t)$ and integrating from an initial time t_0 to t yields

$$\mu(t) V(t) = \mu(t_0) V(t_0) + \frac{C}{\tau} \int_{t_0}^t \mu(s) ds.$$

where $V_0 = V(t_0)$. Solving for $V(t)$, we obtain the general solution

$$V(t) = \mu(t)^{-1} \left[\mu(t_0) V_0 + \frac{C}{\tau} \int_{t_0}^t \mu(s) ds \right], \quad \mu(t) = \exp\left(\frac{1}{\tau} \int_{t_0}^t \kappa(s) ds\right), \quad (20)$$

Thus, for any decay pattern $\kappa(t)$, the flux-limited Keller–Segel system admits an explicit family of X_1 -invariant solutions:

$$u(x, t) = C, \quad v(x, t) = V(t). \quad (21)$$

These solutions describe spatially uniform relaxation dynamics governed entirely by the temporal variation of the chemical decay rate.

5.2 Case II: constant $\kappa(t) = \kappa_0$

5.2.1 Reduction via X_1 (spatially homogeneous)

The symmetry generator $X_1 = \partial_x$ gives spatially homogeneous solutions, so $u_x = v_x = 0$ and we set $u(x, t) = U(t)$, $v(x, t) = V(t)$. The reduced ODE system (11) becomes $U'(t) = 0$ and $\tau V'(t) + \kappa_0 V(t) = U(t)$, so the exact solutions are $U(t) \equiv C$ (constant cell density) and an exponentially relaxing chemical signal $V(t)$ that tends to the steady level $\frac{C}{\kappa_0}$ as $t \rightarrow \infty$.

5.2.2 Reduction via $X_2 = \partial_t$ (steady states)

the invariance condition requires steady-state solutions, so both u and v depend only on space. Substituting $u(x, t) = U(x)$ and $v(x, t) = V(x)$ into the FLKS system with constant decay κ_0 yields the time-independent equations $0 = DU'' - (Uf(V')V)'$ and $0 = V'' - \kappa_0 V + U$, which describe equilibrium spatial patterns where diffusion, flux-limited chemotactic transport, and chemical decay balance each other.

5.2.3 Reduction via $X_1 + \alpha X_2 = \partial_x + \alpha \partial_t$ (traveling waves)

Introducing the traveling coordinate $y = t - \alpha x$ and setting

$$U(y) = u(x, t), \quad V(y) = v(x, t), \quad s(y) = V_y(y). \quad (22)$$

To illustrate the analytical tractability enabled by the Lie symmetry reductions, we now specialize the flux function to the the hyperbolic-tangent limiter. A standard flux-limits (i.e. keeps $|F| \leq V_{\max}$) is

$$F(z) = V_{\max} \tanh\left(\frac{z}{s_0}\right)$$

Using the traveling-wave substitution $y = t - \alpha x$, we obtain

$$v_x = -\alpha V'(y).$$

Hence the flux limiter becomes

$$F(v_x) = V_{\max} \tanh\left(-\frac{\alpha V'(y)}{s_0}\right).$$

Setting $s = V'(y)$, the first equation in system (14) becomes

$$D\alpha^2 U_y - U\left(1 - \alpha V_{\max} \tanh\left(\frac{\alpha s}{s_0}\right)\right) = C_1. \quad (23)$$

Eq. (23) is a linear first-order ODE for U .

Define the integrating factor

$$\mu(y) = \exp\left(-\int^y \frac{1 + \alpha F(-\alpha s(\xi))}{D\alpha^2} d\xi\right). \quad (24)$$

Using the integrating-factor (24), the exact traveling-wave density is

$$U(y) = \mu(y)^{-1} \left[U(y_0)\mu(y_0) + \frac{C_1}{D\alpha^2} \int_{y_0}^y \mu(\eta) d\eta \right]. \quad (25)$$

The second equation in Eq. (14) is

$$\tau V_y = \alpha^2 V_{yy} - \kappa_0 V + U. \quad (26)$$

Differentiating the second equation (26) to eliminate V and substitute U_y , we get

$$\tau s_y = \alpha^2 s_{yy} - \kappa_0 s + U_y, \quad s = V'(y), \quad (27)$$

where $U(y)$ is given explicitly by (25). Eq. (25) together with (27) is the *exact traveling-wave solution* representation for (14) with tanh flux. Exact solution:

$$s(y) = C_1 e^{r_+ y} + C_2 e^{r_- y} + \frac{1}{\alpha^2(r_+ - r_-)} \int_{-\infty}^y \left(e^{r_+(y-\eta)} - e^{r_-(y-\eta)} \right) U'(\eta) d\eta \quad (28)$$

Since $s(y) = V'(y)$, integrate once:

$$V(y) = V_0 + \frac{C_1}{r_+} e^{r_+ y} + \frac{C_2}{r_-} e^{r_- y} + \frac{1}{\alpha^2(r_+ - r_-)} \int_{-\infty}^y \left[\frac{e^{r_+(y-\eta)}}{r_+} - \frac{e^{r_-(y-\eta)}}{r_-} \right] U_y(\eta) d\eta, \quad (29)$$

where constants C_1, C_2, V_0 are fixed by boundedness or far-field conditions (e.g. $V' \rightarrow 0$ as $y \rightarrow \pm\infty$).

Using the traveling-wave ansatz (22), we have

$$y = t - \alpha x, \quad u(x, t) = U(y), \quad v_x(x, t) = -\alpha V'(y) \quad (30)$$

In traveling-wave variables, the flux term in (14) is

$$F(-\alpha V') = F(v_x) = V_{\max} \tanh\left(\frac{v_x}{s_0}\right).$$

Substitute the tanh limiter into (25) and return to (x, t) yields

$$u(x, t) = \mu(t - \alpha x)^{-1} \left[u(t_0, x_0) \mu(y_0) + \frac{C_1}{D\alpha^2} \int_{y_0}^{t-\alpha x} \mu(\eta) d\eta \right], \quad (31)$$

where

$$\mu(y) = \exp\left(-\int_{y_0}^y \frac{1 + \alpha V_{\max} \tanh\left(\frac{v_x(\xi)}{s_0}\right)}{D\alpha^2} d\xi\right), \quad v_x(\xi) := v_x(x, t) \text{ evaluated on } t - \alpha x = \xi.$$

This is the exact *closed-form/quadrature* representation of the cell density in physical coordinates for tanh-limited flux and the reference value $u(t_0, x_0) = U(y_0)$ are fixed by boundary/asymptotic closure. Using the traveling-wave coordinate $y = t - \alpha x$,

$$v(x, t) = V(t - \alpha x) \quad (32)$$

with V given explicitly by (29).

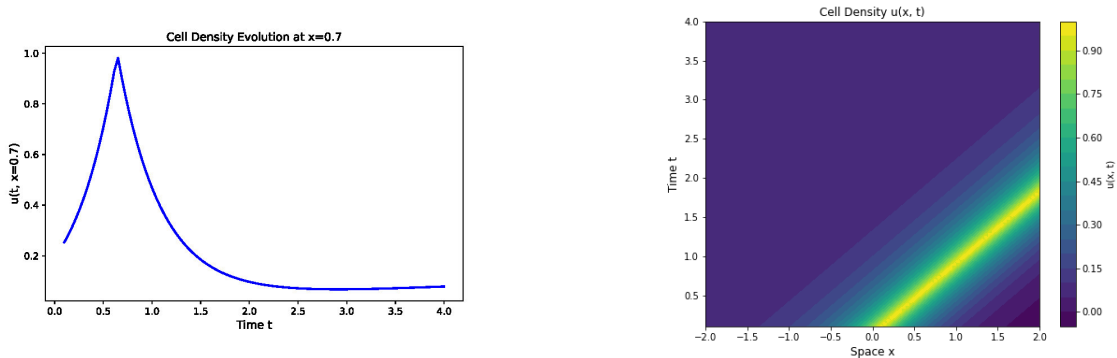


Figure 1: Traveling-wave solution for the cell density in the flux-limited Keller–Segel system with constant decay rate, using the hyperbolic-tangent (tanh) flux limiter. (Left) Temporal evolution of the cell density $u(t)$ at the spatial origin $x = 0.7$, showing a transient increase followed by relaxation due to flux limitation and chemical degradation. (Right) Contour plot of $u(x, t)$, illustrating the propagation of a coherent traveling chemotactic front with finite speed and bounded amplitude. Parameters: $\alpha = 1.1$, $D = 0.8$, $V_{\max} = 1.1$, $s_0 = 1.4$, $A = 2.3$, $\beta = 0.2$, $y_0 = 0$, $u(t_0, x_0) = 1$, $\tau = 0.1$, $\kappa_0 = 0.5$. The solution $u(x, t)$ is given by Eq. (31).

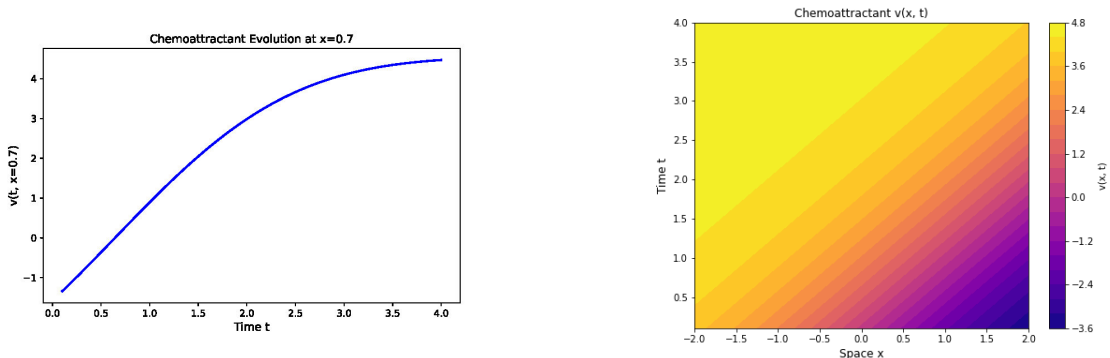


Figure 2: Traveling-wave solution for the chemoattractant field $v(x, t)$ in the flux-limited Keller–Segel system with constant decay rate. (Left) Temporal evolution of the chemoattractant concentration $v(t)$ at the spatial origin $x = 0.7$. $v(x, t)$, reflecting the balance between cellular production and exponential decay. (Right) Contour plot of $v(x, t)$, showing a smooth traveling profile coupled to the migrating cell density and regulated by flux-limited transport. Parameters: $\alpha = 1.1$, $D = 0.8$, $V_{max} = 1.1$, $s_0 = 1.4$, $A = 2.3$, $\beta = 0.2$, $y_0 = 0$, $u(t_0, x_0) = 1$, $\tau = 0.1$, $\kappa_0 = 0.5$. The solution $v(x, t)$ is given by Eq. (32).

Figure 1 and Figure 2 together depict a biologically realistic chemotactic traveling-wave process in which cell migration and signal dynamics are jointly regulated by flux-limited transport and constant chemical degradation. The cell density first rises as cells move up favorable gradients, then saturates smoothly due to the finite motility imposed by flux limitation, producing a coherent, finite-speed wave consistent with observed collective behaviors such as bacterial bands or Dictyostelium streams. This wave ultimately relaxes as directed transport balances continuous chemoattractant decay, showing that sustained aggregation requires ongoing signal production. Correspondingly, the chemoattractant concentration increases gradually and approaches a plateau, reflecting the interplay between cellular production and constant degradation.

5.3 Case III: Power-Law Decay $\kappa(t) = \frac{\mu}{t}$

The inverse-time decay rate $\kappa(t) = \frac{\mu}{t}$ preserves a scaling symmetry and leads naturally to self-similar behaviour. This functional form is compatible with scenarios where signal degradation slows down over time, for instance due to enzyme depletion or adaptation in the degradation pathway.

5.3.1 Reduction via $X_1 = \partial_x$ (spatially homogeneous)

The reduced system (15) yields

$$V'(t) + \frac{\mu}{\tau} \frac{1}{t} V(t) = \frac{C}{\tau}.$$

Introducing the dimensionless parameter $\beta := \frac{\mu}{\tau}$, the integrating factor is t^β , giving

$$\frac{d}{dt}(t^\beta V(t)) = \frac{C}{\tau} t^\beta.$$

case $\mu + \tau \neq 0$ (i.e. $\beta \neq -1$) Integrating from t_0 to t , with $V(t_0) = V_0$ and solving for $V(t)$ yields

$$V(t) = \frac{C}{\mu + \tau} t + \frac{(\mu + \tau)V_0 - Ct_0}{\mu + \tau} \left(\frac{t_0}{t}\right)^{\frac{\mu}{\tau}}.$$

The exact X_1 -invariant solution is

$$u(x, t) = C, \quad v(x, t) = \frac{C}{\mu + \tau} t + \frac{(\mu + \tau)V_0 - Ct_0}{\mu + \tau} \left(\frac{t_0}{t}\right)^{\frac{\mu}{\tau}},$$

where $\mu + \tau \neq 0$.

Special case $\mu = -\tau$ The ODE (15) becomes

$$t^{-1}V(t) = t_0^{-1}V_0 + \frac{C}{\tau} \ln \frac{t}{t_0}.$$

yielding

$$V(t) = \frac{C}{\tau} t \ln \frac{t}{t_0} + \frac{V_0}{t_0} t, \quad (\mu = -\tau),$$

which exhibits a logarithmic growth.

5.3.2 Reduction via X_3 (self-similar scaling)

We introduce the shorthand

$$S(\xi) := V'(\xi),$$

and the dimensionless parameter

$$a := \frac{\Lambda^2}{s_0^2} > 0,$$

with Λ the scale factor from the similarity reduction. For the chemotactic flux we now adopt the bounded tanh-squared limiter

$$F(S) = V_{\max} \tanh(\ln(1 + aS^2)), \quad (33)$$

which satisfies $|F(S)| \leq V_{\max}$ and retains logarithmic sensitivity for small $|S|$.

Differentiating (33) gives

$$F'(S) = V_{\max} \operatorname{sech}^2(\ln(1 + aS^2)) \cdot \frac{2aS}{1 + aS^2}.$$

First integral of the U -equation. Multiplying the U -equation in (16) by the Gaussian integrating factor

$$\mu(\xi) := \exp\left(-\frac{\xi^2}{4D}\right),$$

a direct computation produces an exact divergence identity. Integrating once yields the nonlinear first integral

$$DU'(\xi) - U(\xi) V_{\max} \tanh(\ln(1 + aS(\xi)^2)) = C_1 e^{\xi^2/(4D)} + p e^{\xi^2/(4D)} \int_{\xi} e^{-\eta^2/(4D)} U(\eta) d\eta, \quad (34)$$

where C_1 is an integration constant determined by boundary or asymptotic conditions. Recall the similarity ansatz $u(x, t) = t^p U(\xi)$, $v(x, t) = t^q V(\xi)$ with $\xi = \frac{x}{\sqrt{t}}$, where the exponents p and q are chosen to eliminate explicit t -dependence (here $p = -\frac{1}{2}$, $q = \frac{1}{2}$). The constant p appearing in (34) is the same exponent.

Solving (34) for $U'(\xi)$ gives

$$U'(\xi) = \frac{1}{D} \left\{ U(\xi) V_{\max} \tanh(\ln(1 + aS(\xi)^2)) + C_1 e^{\xi^2/(4D)} + p e^{\xi^2/(4D)} \int_{\xi} e^{-\eta^2/(4D)} U(\eta) d\eta \right\}. \quad (35)$$

Associated linear equation and integrating factor. We may rewrite (35) in the linear form

$$U'(\xi) - \frac{V_{\max}}{D} \tanh(\ln(1 + aS(\xi)^2)) U(\xi) = \frac{C_1}{D} e^{\xi^2/(4D)} + \frac{p}{D} e^{\xi^2/(4D)} \int_{\xi} e^{-\eta^2/(4D)} U(\eta) d\eta.$$

The integrating factor is therefore

$$\mu_e(\xi) = \exp\left(-\frac{1}{D} \int_{\xi} V_{\max} \tanh(\ln(1 + aS(\eta)^2)) d\eta\right).$$

Multiplying through by μ_e and integrating from ξ_0 to ξ yields the exact quadrature

$$U(\xi) = \mu_e(\xi)^{-1} \left\{ U(\xi_0) \mu_e(\xi_0) + \int_{\xi_0}^{\xi} \mu_e(\eta) \left[\frac{C_1}{D} e^{\eta^2/(4D)} + \frac{p}{D} e^{\eta^2/(4D)} \int_{\xi_0}^{\eta} e^{-\zeta^2/(4D)} U(\zeta) d\zeta \right] d\eta \right\}. \quad (36)$$

Differentiated closure equation for $S = V'$. To eliminate V in favor of S , rewrite the second similarity equation in (16) as

$$\tau \left(qV - \frac{\xi}{2} V' \right) = V'' - \mu V + U,$$

differentiate with respect to ξ , and use $V' = S$ and $V'' = S'$ to obtain

$$\tau \left(qS - \frac{\xi}{2} S' \right)' = S'' - \mu S + U'. \quad (37)$$

This provides a closed system for $U(\xi)$ and $S(\xi)$, in which the flux contribution enters through the tanh-squared limiter response (33).

To express the system of equations (36)–(37) in the physical variables (x, t) , we apply the similarity transformations introduced in Section 4.3. The similarity profiles are related to the physical fields through

$$U(\xi) = t^{-p} u(x, t), \quad V(\xi) = t^{-q} v(x, t), \quad \xi = \frac{x}{\sqrt{t}}. \quad (38)$$

Under this transformation, the tanh-squared limiter flux

$$F(S) = V_{\max} \tanh(\ln(1 + aS^2)),$$

is mapped into physical coordinates as

$$F(v_x) = V_{\max} \tanh\left(\ln\left(1 + \frac{v_x^2}{s_0^2}\right)\right), \quad (39)$$

Restricting to the case $C_1 = 0$, the system admits the following representation in physical space. The exact quadrature for the cell density $u(x, t)$ becomes a Volterra integral equation,

$$u(x, t) = \mathcal{E}(x, t) \left[u(x_0, t) \mathcal{E}(x_0, t)^{-1} + \frac{p}{Dt} \int_{x_0}^x \mathcal{E}(y, t)^{-1} e^{\frac{y^2}{4Dt}} \left(\int_{x_0}^y e^{-\frac{z^2}{4Dt}} u(z, t) dz \right) dy \right], \quad (40)$$

where the spatial integrating factor $\mathcal{E}(x, t)$ is induced by the chemotactic gradient and is given by

$$\mathcal{E}(x, t) = \exp\left(\frac{V_{\max}}{D\sqrt{t}} \int_{x_0}^x \tanh(\ln(1 + a t^{1-2q} v_x(y, t)^2)) dy\right), \quad (41)$$

where $q = \frac{1}{2}$.

In physical coordinates, the chemoattractant gradient $v_x(x, t)$ satisfies the following integro-differential equation:

$$\underbrace{(t + \tau x^2) t^{\frac{1}{2}-q} v_{xxx}}_{\text{diffusion}} - \underbrace{\tau \left(q - \frac{1}{2}\right) t^{-q} v_{xx}}_{\text{scaling drift}} - \underbrace{\mu t^{-\frac{1}{2}-q} v_x}_{\text{decay}} + \underbrace{\frac{1}{D} \mathcal{H}[u, v_x]}_{\text{coupling}} = 0. \quad (42)$$

The coupling functional $\mathcal{H}[u, v_x]$ collects the nonlinear flux contribution and the memory term arising from the reduction of the cell density,

$$\mathcal{H}[u, v_x] = t^{-p} u(x, t) V_{\max} \tanh(\ln(1 + a t^{1-2q} v_x(x, t)^2)) + \frac{p}{\sqrt{t}} e^{\frac{x^2}{4Dt}} \int_{x_0}^x e^{-\frac{z^2}{4Dt}} t^{-p} u(z, t) dz. \quad (43)$$

The power-law decay case $\kappa(t) = \frac{\mu}{t}$ occupies a special position in the group classification: it is the only nonconstant decay rate that preserves a dilation symmetry and hence admits self-similar reductions. From both mathematical and biological perspectives, it provides a natural bridge between transient traveling-wave dynamics and long-time diffusive behavior, highlighting the versatility of flux-limited chemotaxis models in capturing realistic signal regulation.

5.4 Case IV: exponential decay $\kappa(t) = \kappa_0 e^{\lambda t}$

For the exponentially time-dependent decay rate

$$\kappa(t) = \kappa_0 e^{\lambda t},$$

the symmetry analysis identifies the generator

$$X_4 = \partial_t - \lambda v \partial_v,$$

which combines time translation with an exponential rescaling of the chemoattractant. This form captures biological situations where signal degradation machinery is up-regulated ($\lambda > 0$) or down-regulated ($\lambda < 0$) at a constant relative rate, e.g. via transcriptional control of degrading enzymes.

5.4.1 Reduction via X_1 (spatially homogeneous dynamics)

For $u(x, t) = U(t)$, $v(x, t) = V(t)$, the reduced system reads

$$\begin{cases} U'(t) = 0, \\ \tau V'(t) + \kappa_0 e^{\lambda t} V(t) = U(t), \end{cases} \quad (44)$$

Thus $U(t) \equiv C$ and

$$V'(t) + \frac{\kappa_0}{\tau} e^{\lambda t} V(t) = \frac{C}{\tau}.$$

Let $a = \kappa_0/(\tau\lambda)$ for $\lambda \neq 0$. The integrating factor is

$$\mu(t) = \exp\left(\frac{\kappa_0}{\tau} \int e^{\lambda t} dt\right) = \exp(ae^{\lambda t}).$$

Integrating from t_0 to t yields

$$\mu(t)V(t) = \mu(t_0)V_0 + \frac{C}{\tau} \int_{t_0}^t \exp(ae^{\lambda s}) ds,$$

and the remaining integral can be expressed in terms of the exponential integral Ei. Thus

$$V(t) = e^{-ae^{\lambda t}} \left[e^{ae^{\lambda t_0}} V_0 + \frac{C}{\tau\lambda} (\text{Ei}(ae^{\lambda t}) - \text{Ei}(ae^{\lambda t_0})) \right]. \quad (45)$$

Equation (45) makes explicit how exponential up-regulation of degradation ($\lambda > 0$) can rapidly extinguish the chemoattractant field, thereby shutting down chemotactic aggregation even at constant cell density. Conversely, $\lambda < 0$ corresponds to progressive weakening of degradation, leading to long-lived chemical signals.

5.4.2 Reduction via X_4 (exponential rescaling of the signal)

We present an exact (quadrature/closed-form) representation of solutions of the X_4 -reduced exponential case equation (18) when the chemotactic flux is of Weber–Fechner type.

Following the X_4 reduction, we consider

$$u(x, t) = U(x, t), \quad v(x, t) = e^{\lambda t} V(x), \quad (46)$$

where we allow U to depend on (x, t) . (Indeed, the factor $e^{-\lambda t} U$ in (18) forces time dependence unless $U \equiv 0$ or $\lambda = 0$; the choice (46) keeps the reduction consistent while avoiding the cell-free restriction.)

Define

$$Z(x, t) := v_x(x, t) = e^{\lambda t} V_x(x). \quad (47)$$

For Weber–Fechner sensing, the flux potential (i.e. the combination that appears in $\partial_x(u f(v_x) v_x)$) is specified by

$$F(Z) := f(Z) Z = V_{\max} \ln\left(1 + \frac{Z^2}{s_0^2}\right). \quad (48)$$

With (46)–(48), the reduced system (18) becomes

$$\begin{aligned} 0 &= D U_{xx}(x, t) - \partial_x(U(x, t) F(Z(x, t))), \\ \tau\lambda V(x) &= V_{xx}(x) - \kappa_0 V(x) + e^{-\lambda t} U(x, t). \end{aligned} \quad (49)$$

This is exactly (18) with the Weber–Fechner choice (48).

Integrating the first equation in (49) once with respect to x yields the exact first integral

$$D U_x(x, t) - U(x, t) F(Z(x, t)) = C_1(t), \quad (50)$$

where $C_1(t)$ is an arbitrary function of time determined by boundary/closure conditions (e.g. prescribed flux, conservation of mass).

Equation (50) may be written as a linear first-order ODE in x :

$$U_x(x, t) - \frac{1}{D} F(Z(x, t)) U(x, t) = \frac{C_1(t)}{D}. \quad (51)$$

Fix a reference point x_0 and define the Integrating factor:

$$\mu(x, t) := \exp\left(-\frac{1}{D} \int_{x_0}^x F(Z(s, t)) ds\right). \quad (52)$$

With (47)–(48), this becomes explicitly

$$\mu(x, t) = \exp\left(-\frac{V_{\max}}{D} \int_{x_0}^x \ln\left(1 + \frac{e^{2\lambda t} V_x(s)^2}{s_0^2}\right) ds\right). \quad (53)$$

Multiplying (51) by μ and integrating from x_0 to x gives the exact quadrature solution

$$U(x, t) = \mu(x, t)^{-1} \left[U(x_0, t) \mu(x_0, t) + \frac{C_1(t)}{D} \int_{x_0}^x \mu(s, t) ds \right]. \quad (54)$$

Substituting (54) into the second equation of (49) yields

$$V_{xx}(x) - (\kappa_0 + \tau\lambda)V(x) = -e^{-\lambda t} \mu(x, t)^{-1} \left[U(x_0, t) \mu(x_0, t) + \frac{C_1(t)}{D} \int_{x_0}^x \mu(s, t) ds \right]. \quad (55)$$

Since the left-hand side of (55) depends only on x , the right-hand side must be t -independent. Therefore, Eq. (55) is valid only under an additional compatibility condition ensuring that the factors $e^{-\lambda t}$, $\mu(x, t)$, and $C_1(t)$ combine to produce a purely spatial expression.

Equivalently, V satisfies the exact integro-differential closure

$$\tau\lambda V(x) = V_{xx}(x) - \kappa_0 V(x) + e^{-\lambda t} \mu(x, t)^{-1} \left[U(x_0, t) \mu(x_0, t) + \frac{C_1(t)}{D} \int_{x_0}^x \mu(s, t) ds \right], \quad (56)$$

where μ is given by (53) and depends on V_x . Thus, the only nonlinearity enters through the single spatial integral inside μ .

5.4.3 Reduction via $X_1 + \alpha X_4$

The generator

$$X = X_1 + \alpha X_4 = \partial_x + \alpha \partial_t - \alpha \lambda v \partial_v$$

describes traveling waves coupled to an exponential rescaling of v . The characteristic equations

$$\frac{dx}{1} = \frac{dt}{\alpha} = \frac{dv}{-\alpha \lambda v}$$

yield the invariants

$$y = t - \alpha x, \quad v e^{\lambda t} = \Phi(y),$$

Therefore, we take

$$u(x, t) = U(y), \quad v(x, t) = e^{-\lambda t} V(y), \quad y = t - \alpha x.$$

The system (19) for the traveling wave with $\lambda \neq 0$ is not a set of ODEs and therefore has no simple closed-form solution. For cell-free states $U(y) \equiv 0$, the reduced equation for V becomes

$$\alpha^2 V_{yy} - \tau V_y - (\kappa_0 - \tau \lambda) V = 0.$$

This has exponential solutions

$$V(y) = Ae^{r_1 y} + Be^{r_2 y}, \quad r_{1,2} = \frac{\tau \pm \sqrt{\tau^2 + 4\alpha^2(\kappa_0 - \tau \lambda)}}{2\alpha^2},$$

and thus

$$v(x, t) = e^{-\lambda t} (Ae^{r_1(t-\alpha x)} + Be^{r_2(t-\alpha x)}).$$

These solutions describe traveling chemical fronts whose amplitude is simultaneously modulated by exponential decay or growth. Biologically, they model chemotactic cues that propagate with a well-defined wave speed while being globally damped (for $\lambda > 0$) or amplified (for $\lambda < 0$), for example during wave-like cAMP signalling in developing *Dictyostelium* under time-varying phosphodiesterase activity [1, 8, 19].

6 Conclusion

We have performed a complete group classification of the one-dimensional flux-limited Keller–Segel system with time-dependent chemical decay rate $\kappa(t)$, employing equivalence transformation theory to systematically identify all admissible Lie symmetry algebras. Our analysis establishes that arbitrary decay functions admit only the spatial translation symmetry $X_1 = \partial_x$, while three distinguished cases extend this kernel algebra: constant decay $\kappa(t) = \kappa_0$, inverse-time power-law decay $\kappa(t) = \mu/t$, and exponential decay $\kappa(t) = \kappa_0 e^{\lambda t}$. For each case, we constructed optimal systems of one-dimensional sub-algebras and derived the corresponding similarity reductions, yielding spatially homogeneous relaxation dynamics, steady-state patterns, traveling waves, and self-similar profiles. Explicit analytical solutions were obtained for the constant and exponential decay cases using the hyperbolic-tangent flux limiter, demonstrating the practical utility of the symmetry-based approach.

The explicit solutions derived for different temporal decay laws clarify how biochemical regulation of signal degradation shapes collective behavior. Constant decay supports bounded traveling fronts and stable aggregation patterns, corresponding to situations in which chemoattractant production and degradation are balanced. Power-law decay naturally leads to self-similar redistribution of cells and signals, suggesting that slowly weakening degradation mechanisms can sustain long-range communication and coordinated migration over extended times. Exponential decay or amplification, on the other hand, can rapidly suppress or enhance chemotactic cues, providing a plausible mechanism for biological systems to switch aggregation processes on or off through enzymatic or genetic regulation of degradation pathways.

Our results demonstrate that time-dependent chemical decay and flux limitation are not merely mathematical regularizations but encode biologically meaningful control strategies. The symmetry classification presented here provides a rigorous mathematical foundation for understanding which temporal decay patterns admit similarity reductions, thereby enabling analytical progress on flux-limited chemotaxis models with realistic time-varying degradation mechanisms.

Remark 1 *The self-similar reduction for the power-law decay case $\kappa(t) = \mu/t$ leads to an integro-differential system that does not admit a purely local ordinary differential equation reduction under generic flux-limiting functions. The explicit solution formulas presented for this case should therefore be interpreted as a formal representation that requires additional closure assumptions or numerical integration. A complete analysis of this case remains an open direction for future investigation.*

References

- [1] Alber, Andrea Brigitta, and David Michael Suter. Dynamics of protein synthesis and degradation through the cell cycle. *Cell Cycle* 18, no. 8 (2019): 784–794.

- [2] Bader, Sonya, Arjan Kortholt, and Peter J. M. Van Haastert. Seven Dictyostelium discoideum phosphodiesterases degrade three pools of cAMP and cGMP. *Biochemical Journal* 402, no. 1 (2007): 153–161.
- [3] M. Bazghandi, A Symmetry-Based Study of Nonlocal Structures in the Modified Benjamin–Bona–Mahony Equation, *Eur. Phys. J. Plus* 141, (2026): 470.
- [4] Carrillo, José Antonio, Sabine Hittmeir, and Ansgar Jüngel. Cross diffusion and nonlinear diffusion preventing blow-up in the Keller–Segel model. *Mathematical Models and Methods in Applied Sciences* 22, no. 12 (2012): 1250041.
- [5] Chertock, Alina, Alexander Kurganov, Xuefeng Wang, and Yaping Wu. On a chemotaxis model with saturated chemotactic flux. *Kinetic and Related Models* 5, no. 1 (2012): 51–95.
- [6] Erban, Radek, and Hans G. Othmer. From individual to collective behavior in bacterial chemotaxis. *SIAM Journal on Applied Mathematics* 65, no. 2 (2004): 361–391.
- [7] R. K. Gazizov, A. A. Kasatkin, and S. Y. Lukashchuk, “Group classification and symmetry reduction of three-dimensional nonlinear anomalous diffusion equation,” *Ufimskij Matem. Zhurn*, vol.11, no.4 (2019): 14–28.
- [8] Golding, Ido, Johan Paulsson, Scott M. Zawilski, and Edward C. Cox. Real-time kinetics of gene activity in individual bacteria. *Cell* 123, no. 6 (2005): 1025–1036.
- [9] Haghghatdoost, Ghorbanali, and Mustafa Bazghandi. Lie symmetry analysis and similarity reductions for the tempered-fractional Keller–Segel system. *arXiv preprint arXiv:2509.11690* (2025).
- [10] G. Haghghatdoost, M. Bazghandi, and F. Pashaie. Differential Invariants of coupled Hirota–Satsuma KDV Equations, *Kragujev. J. Math.*, 49(5) (2025): 793–805.
- [11] Hillen, Thomas, and Kevin J. Painter. A user’s guide to PDE models for chemotaxis. *Journal of Mathematical Biology* 58, no. 1 (2009): 183–217.
- [12] Hittmeir, Sabine, and Ansgar Jüngel. Cross diffusion preventing blow-up in the two-dimensional Keller–Segel model. *SIAM Journal on Mathematical Analysis* 43, no. 2 (2011): 997–1022.
- [13] Ivanova, N. M., and C. Sophocleous. On the group classification of variable coefficient nonlinear diffusion–convection equations. *Journal of Computational and Applied Mathematics* 197 (2006): 322–344.
- [14] Ivanova, N. M., R. O. Popovych, and C. Sophocleous. Group analysis of variable coefficient diffusion–convection equations. I. Enhanced group classification. *Lobachevskii Journal of Mathematics* 31 (2010): 100–122.
- [15] Jaiswal, Anjali, Poonam Rani, and Jagmohan Tyagi. Global weak solutions of a parabolic–elliptic Keller–Segel system with gradient dependent chemotactic coefficients. *Discrete and Continuous Dynamical Systems – Series B* 28, no. 7 (2023).
- [16] Kalinin, Yevgeniy V., Lili Jiang, Yuhai Tu, and Mingming Wu. Logarithmic sensing in *Escherichia coli* bacterial chemotaxis. *Biophysical Journal* 96, no. 6 (2009): 2439–2448.
- [17] Kohatsu, Shohei, and Takasi Senba. Critical mass and stability of radial steady states for a flux-limited Keller–Segel system in the critical case. *Nonlinearity* 38, no. 9 (2025): 095006.
- [18] Kohatsu, Shohei, and Takasi Senba. Self-similar solutions to a flux-limited Keller–Segel system. *Nonlinear Analysis: Real World Applications* 84 (2025): 104308.
- [19] Lenstra, Tineke L., Joseph Rodriguez, Huimin Chen, and Daniel R. Larson. Transcription dynamics in living cells. *Annual Review of Biophysics* 45, no. 1 (2016): 25–47.
- [20] Maini, Philip K. Using mathematical models to help understand biological pattern formation. *Comptes Rendus Biologies* 327, no. 3 (2004): 225–234.

- [21] Opanasenko, Stanislav, Alexander Bihlo, and Roman O. Popovych. Group analysis of general Burgers–Korteweg–de Vries equations. *Journal of Mathematical Physics* 58, no. 8 (2017).
- [22] Ovsianikov, L. V. Group relations of the equation of non-linear heat conductivity. *Doklady Akademii Nauk SSSR* 125, no. 3 (1959): 492–495.
- [23] Painter, Kevin J. Mathematical models for chemotaxis and their applications in self-organisation phenomena. *Journal of Theoretical Biology* 481 (2019): 162–182.
- [24] Palsson, Eirikur, and Edward C. Cox. Origin and evolution of circular waves and spirals in *Dictyostelium discoideum* territories. *Proceedings of the National Academy of Sciences* 93, no. 3 (1996): 1151–1155.
- [25] Perthame, Benoît, Nicolas Vauchelet, and Zhian Wang. The flux-limited Keller–Segel system: properties and derivation from kinetic equations. *Revista Matemática Iberoamericana* 36, no. 2 (2019): 357–386.
- [26] Popovych, R. O., and N. M. Ivanova. New results on group classification of nonlinear diffusion–convection equations. *Journal of Physics A: Mathematical and General* 37 (2004): 7547–7565.
- [27] Xiang, Tian. Sub-logistic source can prevent blow-up in the 2D minimal Keller–Segel chemotaxis system. *Journal of Mathematical Physics* 59, no. 8 (2018).
- [28] Zeng, Ziyue, Jianlu Yan, and Yuxiang Li. Boundedness and finite-time blow-up in a repulsion-consumption system with flux limitation. *Journal of Mathematical Physics* 66, no. 9 (2025).